First detection of ^{13}CH in the ISM

A. M. Jacob , K. M. Menten, H. Wiesemeyer, R. Güsten, F. Wyrowski
& B. Klein
Max Planck Institute for Radioastronomy, Bonn

(A&A 640, A125, 2020)

Sgr B2

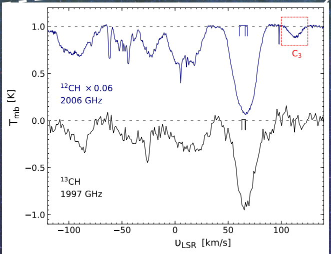

SOFIA Community Tele-Talk
October 7, 2020

Background Image: GLIMPSE/Spitzer IR image (Churchwell+06)

Isotopic abundance ratios

Carbon-12 (^{12}C):

- Primary product of stellar nucleosynthesis
- He-burning via triple α-reaction

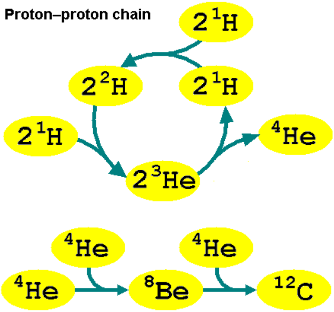

Isotopic abundance ratios

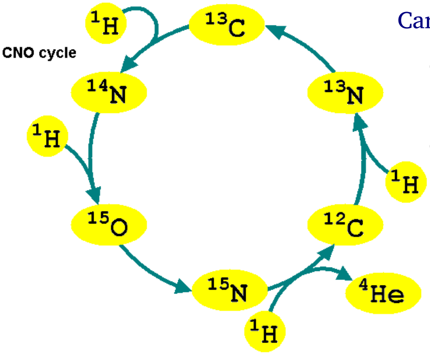

Carbon-13 (^{13}C):

- Secondary product of stellar nucleosynthesis
- By-product of the CNO-cycle

Isotopic abundance ratios

Carbon-12 (^{12}C):

- Primary product of stellar nucleosynthesis
- He-burning via triple α-reaction

Carbon-13 (^{13}C):

- Secondary product of stellar nucleosynthesis
- By-product of the CNO-cycle

^{12}C/^{13}C isotopic ratio $\Rightarrow$ primary/secondary processing

Essential diagnostic of the history of Galactic nucleosynthesis and chemical enrichment

Models and observations

$^{12}C/^{13}C$ model predictions

(e.g. Tosi 1982)

- Increase with R_{GC}
- Star-formation rates higher toward the Galactic centre

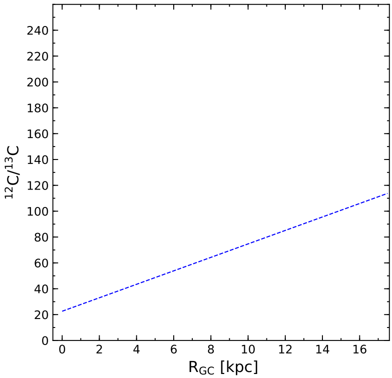

Models and observations

$^{12}C/^{13}C$ model predictions

(e.g. Tosi 1982)

- Increase with R_{GC}
- Star-formation rates higher toward the Galactic centre

Observations

- Reveals a positive gradient
- H_2CO (Henkel et al. 1985, Yan et al. 2019)

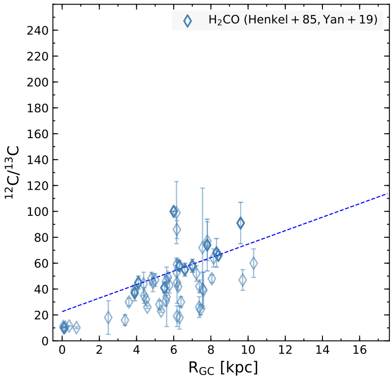

Models and observations

$^{12}C/^{13}C$ model predictions

(e.g. Tosi 1982)

- Increase with R_{GC}
- Star-formation rates higher toward the Galactic centre

Observations

- Reveals a positive gradient
- H_2CO (Henkel et al. 1985, Yan et al. 2019)
- CO, $C^{18}O$ (Langer & Penzias 1990,Wouterloot & Brand 1996, Giannetti et al. 2014)
- CN (Savage et al. 2002, Milam et al. 2005); CH^+ (Ritchey et al. 2011); Complex organic molecules (COMs) (Halfen et al. 2017)

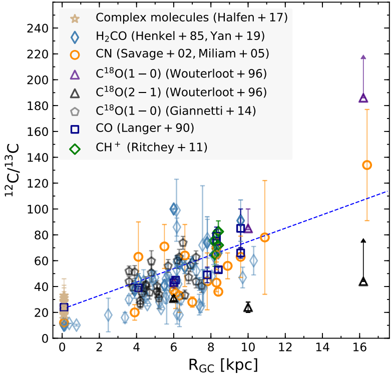

Challenges in interpretation

H_2CO ; Henkel et al. 1982

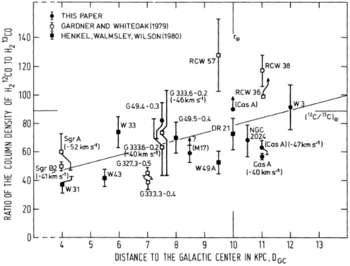

CO ; Langer & Penzias 1990

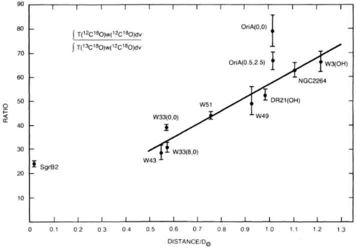

Systematic variations and scatter amongst molecules

Why are there inconsistencies?

- Observational effects
- Isotope selective processes

Isotope selective processes

Chemical fractionation

- Due to small differences in binding energy
  $\Rightarrow$ small differences in zero-point energies
  $\Rightarrow$ differences in mass

- For example:

  $^{13}C^{+} + CO \rightarrow C^{+} +^{13} CO + 35$ K

  Enriches ^{13}C isotope

  Extend of fractionation varies in different species

Selective photo-dissociation

- UV-dominant regions (diffuse/translucent clouds)
- Decreases ^{13}C
- Weaker self-shielding of ^{13}C isotope

The promise of CH^+(?)

$C^+ \xrightarrow[H_2+h\nu]{H} CH^+$; ($\Delta E$ = 4640 K) $\Rightarrow$ Unaffected by fractionation

- CH^+ 4232 Å (Ritchey et al. 2011)

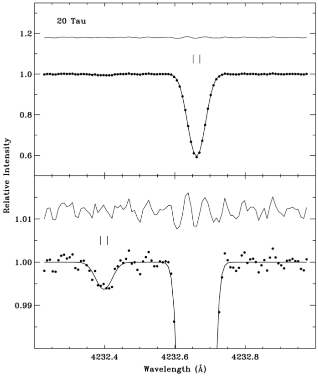

$\Rightarrow$ Limited to nearby (<7 kpc), bright (V<10 mag) sources

- CH^+ 830 GHz (Godard et al. 2012)

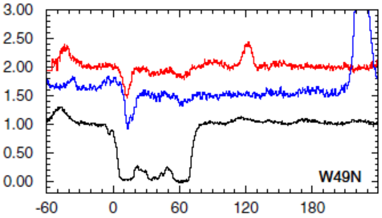

Saturated CH^+ absorption!

$\Rightarrow$ Lower limit on the $^{12}C/^{13}C$ ratio

Aim

- Using different species ⇒ can reveal systematics in $^{12}C/^{13}C$
- But optical depth effects, fractionation, selective photo-dissociation ⇒ measurement biases

What does the underlying $^{12}C/^{13}C$ look like?

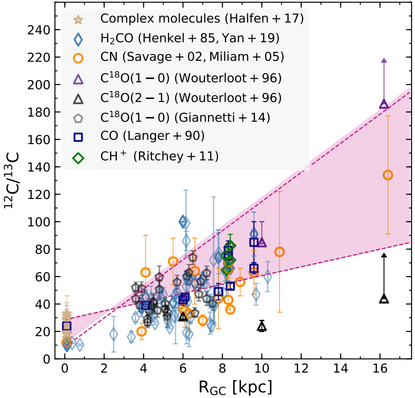

A new tracer - CH

- One of the first molecules to be detected in the ISM

  (Dunham 1937)

- Early product of chemical network

  $\Rightarrow$ Building block of larger molecules

$$C^+ \xrightarrow{H_2} CH_2^+ \xrightarrow{H_2} CH_3^+ \xrightarrow{e^-} CH$$

$$C^+ \xrightarrow[H_2+h\nu]{H} CH^+ \xrightarrow[H_2+h\nu]{H} CH_2^+ \xrightarrow{e^-} CH$$

(Turbulence driven chemistry)

CH lines are almost ALWAYS optically thin!
At all wavelengths (optical, FIR, sub-mm and radio)!

Problem: ^{13}CH has not yet been detected in the ISM

Energy level diagram

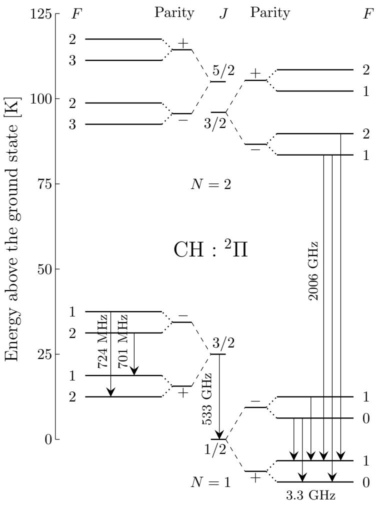

(Note: Energy levels are not to scale)

- CH 3.3 GHz ⇒ anomalous excitation

  Difficult to interpret

- CH 533/537 GHz

  Complex spectra (ems+abs), standing waves, line contamination

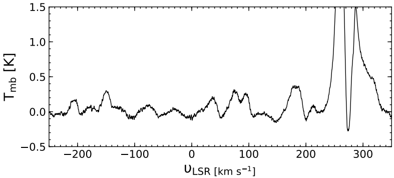

Observational setup

German **RE**ceiver for **A**stronomy at **T**erahertz frequencies

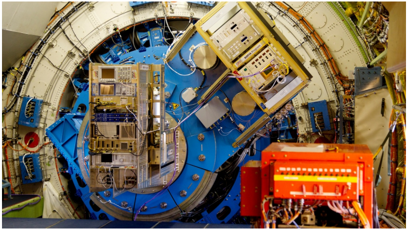

Credits: Deutsches SOFIA Institut

- High resolution
  → Spectral resolution of 244 kHz
- Six frequency channels
  0.49-4.74 THz
- Multi-pixel, heterodyne spectrometer
- Available in two configurations
  LFA + HFA
  4G + HFA

(Risacher et al. 2018)

Duran et. al 2020 (submitted IEEE THz)

Channels		Frequency [THz]	Trec Double Sideband [K]	FWHM [´´]
upGREAT	HFA	4.7447	1250	6.3
	LFA-H	1.835–2.007	1000	14.1
	LFA-V	1.835–2.007 2.060–2.065	1000	14.1
4GREAT	4G4	2.480–2.620	3300	10.5
	4G3	1.240–1.395 1.425–1.525	1100	20
	4G2	0.850–0.975 0.990–1.085	>600	27
	4G1	0.495–0.550 0.563–0.630	300	52

CH observations (Wiesemeyer et al. 2018, Jacob et al. 2019)

CH $(N, J = 2, 3/2 \rightarrow 1, 1/2)$

Example toward Sgr B2(M)

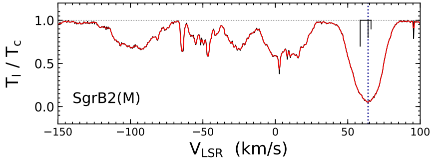

Frequencies from Davidson et al. 2001

Parity	Transition F' - F''	Frequency [GHz]	A_E 10^{-2}x $[s^{-1}]$
- → +	1 – 1	2006.74892	1.117
	1 – 0	2006.76263	2.234
	2 – 1	2006.79912	3.351
+ → -	1 – 1	2010.73859	1.128
	1 – 0	2010.81046	2.257
	2 – 1	2010.81192	3.385

CH observations (Wiesemeyer et al. 2018, Jacob et al. 2019)

CH $(N, J = 2, 3/2 \rightarrow 1, 1/2)$

Frequencies from Davidson et al. 2001

Parity	Transition F' - F''	Frequency [GHz]	A_E 10^{-2}x [s^{-1}]
- → +	1 – 1	2006.74892	1.117
	1 – 0	2006.76263	2.234
	2 – 1	2006.79912	3.351
+ → -	1 – 1	2010.73859	1.128
	1 – 0	2010.81046	2.257
	2 – 1	2010.81192	3.385

Example toward Sgr B2(M)

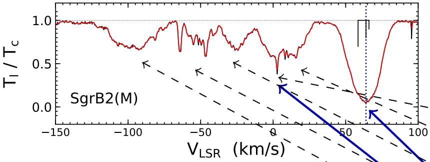

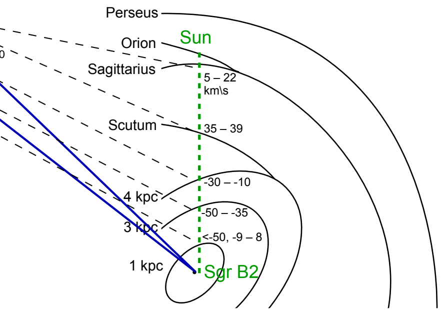

Sketch of spiral arms along the sight line toward Sgr B2(M) based on Greaves & Williams, 1994

^{13}CH observations

- Observation strategy:

  Strong continuum sources

  Cover a range of R_{GC}

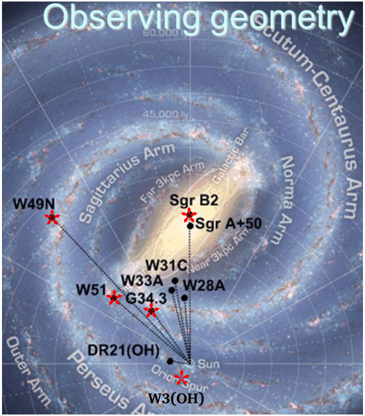

Frequencies from Davidson et al. 2004

Parity	Transition F' - F"	Frequency [GHz]	A_E 10^{-3}x [s^{-1}]
- → +	1,3/2 – 0,1/2	1997.4232	1.146
	1,3/2 – 1,3/2	1997.4464	0.573
	2,5/2 – 1,3/2	1997.4437	1.909
+ → -	1,3/2 – 0,1/2	2001.5672	1.157
	1,3/2 – 1,3/2	2001.2231	0.578
	2,5/2 – 1,3/2	2001.3673	1.929

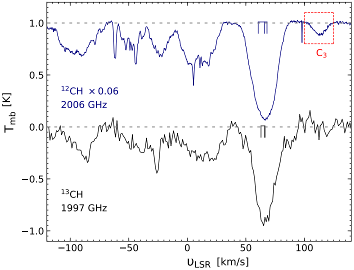

Sideband deconvolution ⇒

For disentangling sight line features from contamination

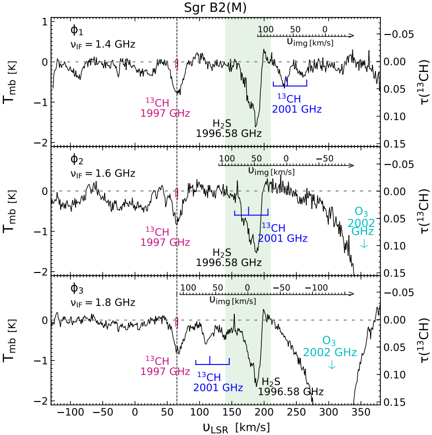

- Three different IF settings (e.g. IF = 1.2, 1.4 and 1.6 GHz)
- DSB spectrum

$$\phi(\upsilon)_i = \phi_{\text{sig}}(\upsilon) + \phi_{\text{img}}(\upsilon_i - \upsilon)$$

- Average

$$\phi(\upsilon)_{\text{avg}} = \phi_{\text{sig}}(\upsilon) + \sum_{i=1}^{3} \phi_{\text{img}}(\upsilon_i - \upsilon)/3$$

- Residuals

$$\phi(\upsilon)_{1-2}, \phi(\upsilon)_{1-3}$$

- Average of residuals

$$\left(\phi(\upsilon)_{1-2} + \phi(\upsilon)_{1-3}\right)/2$$

- Resultant spectrum = Average - Average of residuals

Sideband deconvolution

Sideband deconvolution ⇒

For disentangling sight line features from contamination

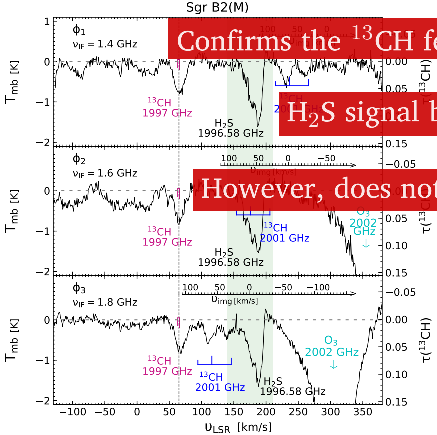

- Three different IF settings (e.g. IF = 1.2, 1.4 and 1.6 GHz)
- DSB spectrum

  $\phi(\upsilon)_i = \phi_{\text{sig}}(\upsilon) + \phi_{\text{img}}(\upsilon_i - \upsilon)$
- Average

  $\phi(\upsilon) = \phi_{\text{sig}}(\upsilon) + \sum_{i=1}^{3} \phi_{\text{img}}(\upsilon_i - \upsilon)/3$
- Residuals

  $\phi(\upsilon)_{1-2}, \phi(\upsilon)_{1-3}$
- Average of residuals

  $\left(\phi(\upsilon)_{1-2} + \phi(\upsilon)_{1-3}\right)/2$
- Resultant spectrum = Average - Average of residuals

Confirms the ^{13}CH features from both sidebands

H_2S signal band contamination

However, does not confirm the LOS features

Results toward other sources I

G34.26+0.15

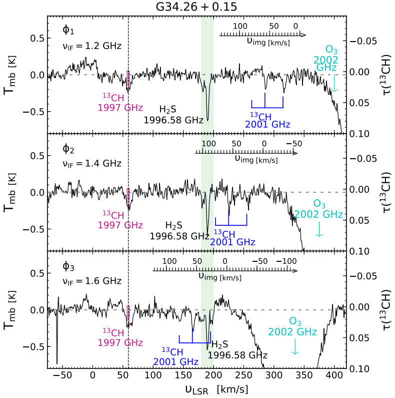

W49N

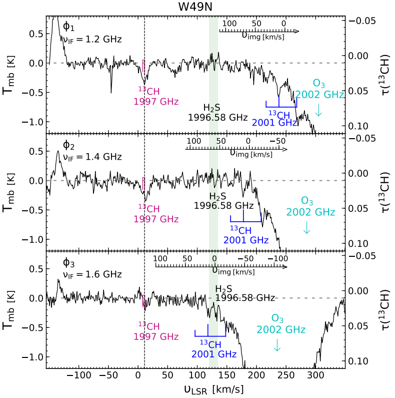

Results toward other sources II

W51E

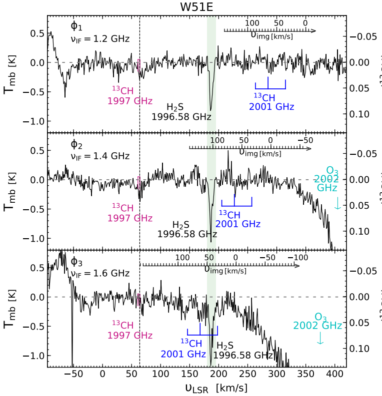

W3(OH)

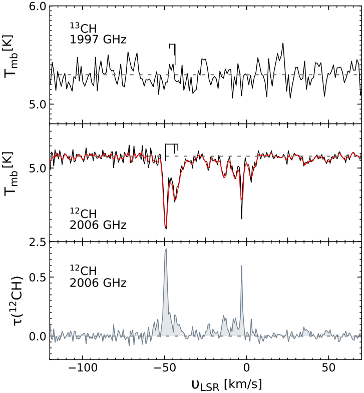

Analysis I

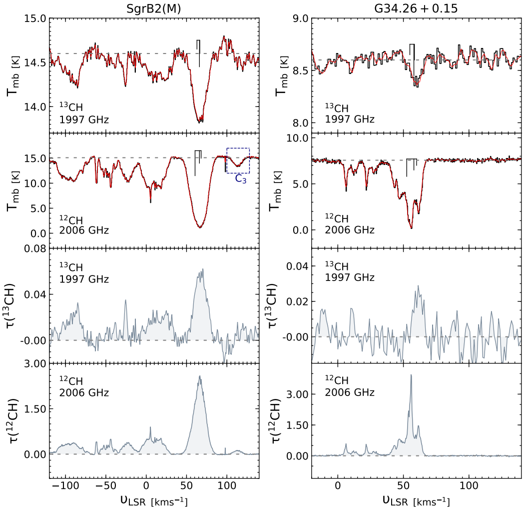

- Fit using Wiener filter deconvolution algorithm (Jacob et al. 2019)
- Deconvolves hyperfine structure from observed spectrum in Fourier space

  ⇒ Reveal underlying "original" spectrum

Analysis II

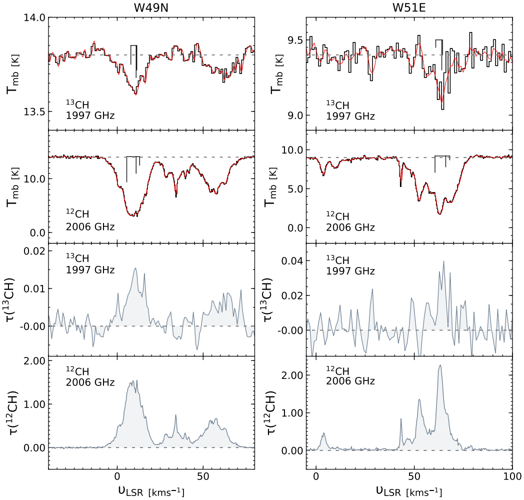

- From the absorption spectra we can directly derive column densities

Analysis II

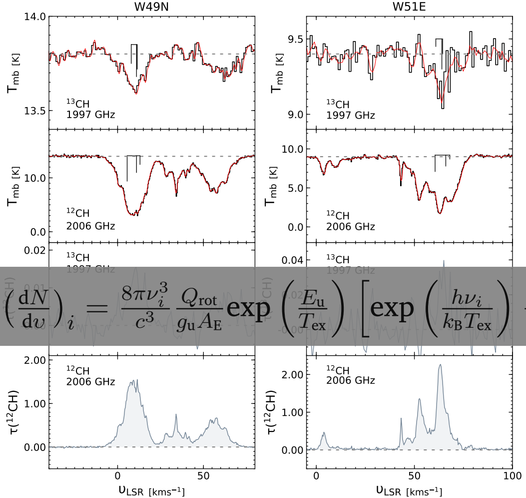

$$\left(\frac{\mathrm{d}N}{\mathrm{d}\upsilon}\right)_i = \frac{8\pi\nu_i^3}{c^3}\frac{Q_{\mathrm{rot}}}{g_{\mathrm{u}}A_{\mathrm{E}}}\exp\left(\frac{E_{\mathrm{u}}}{T_{\mathrm{ex}}}\right)\left[\exp\left(\frac{h\nu_i}{k_{\mathrm{B}}T_{\mathrm{ex}}}\right)-1\right]^{-1}\left(\tau_{\mathrm{decon}}\right)_i$$

- From the absorption spectra we can directly derive column densities

Results

Source	$N(^{13}CH)$ [10^{13} cm^{-2}]	$N(^{12}CH)$ [10^{13} cm^{-2}]	$^{12}C/^{13}C$ CH	CN	R_{GC} [kpc]
SgrB2(M)	4.61	73.02	15.8	>12	0.1
W51E	1.77	66.36	37.5	35	6.3
G34.26+0.15	0.2	9.38	47	28	7
W49(N)	0.68	22.87	33.6	44	7.8
W3(OH)	<0.11	6.58	>58	63	10

- $^{12}C/^{13}C$ similar for both CH and CN (Milam et al. 2005)
- CH + N $\rightarrow$ CN + H
- Discrepancy for G34.26+0.15 $\Rightarrow$ ^{12}CN shows non-LTE effects
- $^{12}C/^{13}C$ from complex organic molecules (COMs) (Halfen et al. 2017) average value for GC $\sim 24 \pm 9$

  $\Rightarrow$ similarities within errors
  $\Rightarrow$ ^{13}C substitution derives from early stage molecules like CH and CN

Revised $^{12}C/^{13}C$ Galactic gradient

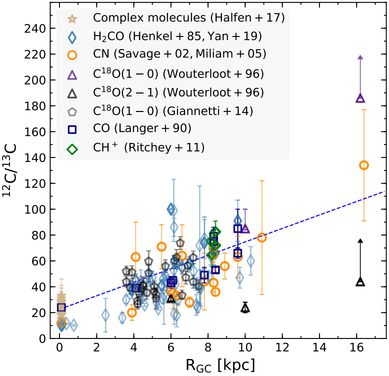

Revised $^{12}C/^{13}C$ Galactic gradient

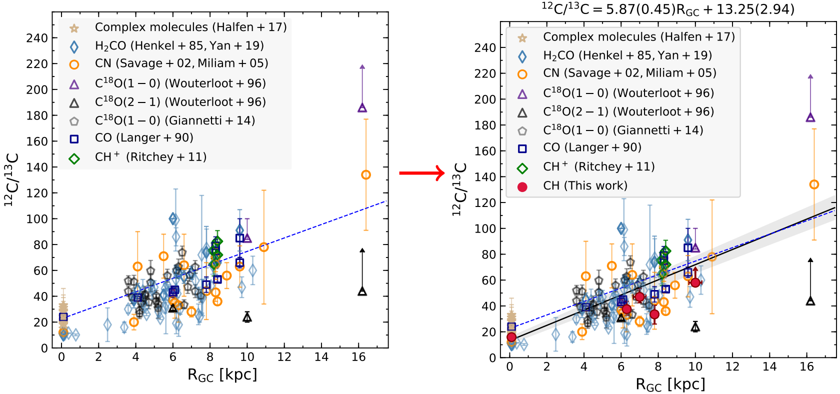

$$^{12}\mathbf{C}/^{13}\mathbf{C} = 5.85(0.50)\ R_{\mathbf{GC}} + 15.03(3.40)$$

Summary

- First detection of ^{13}CH in the ISM
- Smaller uncertainties in CH column densities
  - $\Rightarrow$ Smaller errors in the overall fit
  - $\Rightarrow$ New constraints on Galactic chemical evolution models
- CH relatively unaffected by fractionation effects
  - $\Rightarrow$ low $A_{\rm v}$ regions
  - $\Rightarrow$ Turbulence/ UV-driven chemistry
- ^{13}C substitution in CH $\Rightarrow$ Important in chemistry

Future prospects

- Promote laboratory studies of other ^{13}CH transitions
- Extend the search for ^{13}CH in other sources and hunt for other ^{13}CH transitions

Thank you

Backup: Wiener filter algorithm (Jacob et al. 2019)

$$F(\nu) = \frac{D(\nu)}{H(\nu)} \frac{|H(\nu)|^2}{|H(\nu)|^2 + |1/(S/R)|^2}$$